AIAA JOURNAL
Vol. 44, No. 11, November 2006

Multiple Crack Analysis in Finite Plates

A. Kadir Yavuz* and S. Leigh Phoenix†
Cornell University, Ithaca, New York 14853
and
Stephanie C. TerMaath‡
Applied Research Associates, Inc., Fort Worth, Texas 76109

DOI: 10.2514/1.17919

In this study, interactions of multiple cracks in finite rectangular plates are analyzed. A finite plate is treated as a polygon-shaped plate which can be created by contiguous crack segments embedded in an infinite plate forming an enclosed region so there are no true crack tips remaining around the plate. This boundary value problem is solved with the superposition approach based on the dislocation distributions requiring the determination of crack opening displacement profiles that satisfy the traction-free condition on interior crack faces and the given boundary tractions on four exterior cracklike segments defining the outside boundary of the rectangular plate. A new point allocation scheme that reduces the number of evaluation points leads to a set of linear algebraic equations in terms of unknown weighting coefficients of opening displacement profiles involving polynomial terms and wedge terms whose exponents are approximated as rational numbers to represent irrational wedge eigenvalues, thus permitting evaluation of the integrals in closed form. Then, stress and displacement fields on the entire body, as well as the usual stress intensity factors at the crack tips and kinks, are calculated. The accuracy of the method and the strong interactions of multiple cracks are demonstrated with figures and tables.

Nomenclature

a_i	=	length of ith crack segment
C	=	number of crack segments
G	=	shear modulus
$K_{I,II}$	=	mode I and II stress intensity factors, respectively
N	=	number of polynomial and wedge terms
n	=	number of allocation points for each set
p, w	=	weighting coefficients of polynomial and wedge terms, respectively
$P(t)$, $W(t)$	=	polynomial and wedge series, respectively
κ	=	Kosolov's constant
μ	=	dislocation distribution
ν	=	Poisson's ratio
ρ	=	wedge eigenvalue
$\sigma_{x,y,xy}$	=	normal and shear stress components
$\sigma^*_{XX,YY,XY}$	=	prescribed normal and shear stress components on plate boundaries

I. Introduction

DEVELOPMENT of analysis methods to calculate the stresses around multiple cracks in elastic solids has been an important but difficult research problem for many decades. Interaction effects among cracks is an important factor in aging of such structures as aerospace fuselages and marine hulls, as well as damage evolution in poly-crystalline and multiphase materials in general. An important fact is that in an array of cracks, the strengths of the interactions are strongly dependent on their local geometry, placement, and orientation. Interactions which do not adversely affect stiffness may greatly reduce strength and fatigue life.

The current study is focused on analyzing interactions of multiple cracks in *finite* plates. The solution method we use is an extension to finite plates of the technique (without using constraints and with changed polynomial structures) developed by Burton and Phoenix [1] for two-dimensional problems for infinite plates and modified by TerMaath [2], TerMaath et al. [3], and Yavuz et al. [4]. We generate some specific results for 2-D problems to compare to published results for finite plates [5] and recent approximate solution techniques, which are the modified Kachanov method (MKM) [6], finite element method (FEM) [7], and boundary element method (BEM) [8]. The efficiency and accuracy of the method is demonstrated using tables. This study shows that the method may well be the fastest one among the other methods such as MKM, BEM, and FEMs in calculating stress intensity factors (SIFs) in multicrack elasticity problems for both infinite and finite plates of this type. All presented problems are solved in a short time (for example, it takes less than 1 min to calculate SIFs for the problem of three collinear cracks in a finite plate involving 10 crack segments in Fig. 1) by MATLAB (Release 14) with a notebook PC (Intel Pentium 4, 2.4 GHz CPU, 512 MB RAM).

The first task will be to summarize the theory of dislocation-based influence fields and to explain the particular application procedure for finite plates. The accuracy of the method is shown by comparing the results from different sample problems in a finite rectangular plate. Afterwards, strong interactions of multiple cracks in finite plates will be demonstrated under various loading conditions. These cracks will consist of single straight and skewed cracks, branched Y-cracks, and kinked V-cracks, with results presented in figures and tables.

II. Solution Procedure

A finite plate is treated as a polygon-shaped plate which can be created by contiguous cracklike segments embedded in an infinite plate and forming an enclosed region; thus there are no true crack tips remaining around the plate boundary (Fig. 1). Unlike the interior cracks in the polygon-shaped plate, which are normally traction-free, tractions must be specified on the circumferential boundary crack segments or "cuts" to create the correct stresses and strains in the

Presented as Paper 2322 at the 46th AIAA/ASME/ASCE/AHS/ASC Structures, Structural Dynamics & Materials Conference, Austin, TX, 18–21 April 2005; received 28 May 2005; revision received 6 March 2006; accepted for publication 8 March 2006.

*Research Associate, Theoretical and Applied Mechanics, 111 Thurston Hall. Member AIAA.
†Professor, Theoretical and Applied Mechanics, 321 Thurston Hall.
‡Senior Engineer, 6320 Southwest Boulevard, Suite 103. Member AIAA.

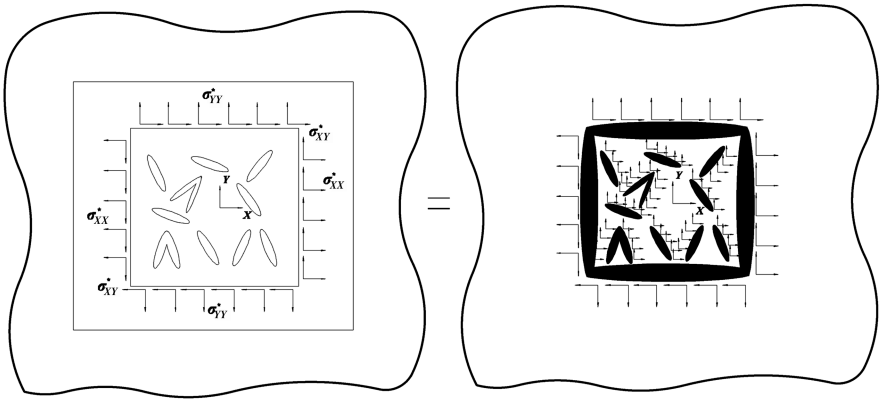

Fig. 1 Definition of boundary value problem for multiple cracks in a finite plate viewed as a rectangular "cutout" in an infinite plate with tractions chosen to match those on the finite plate of interest.

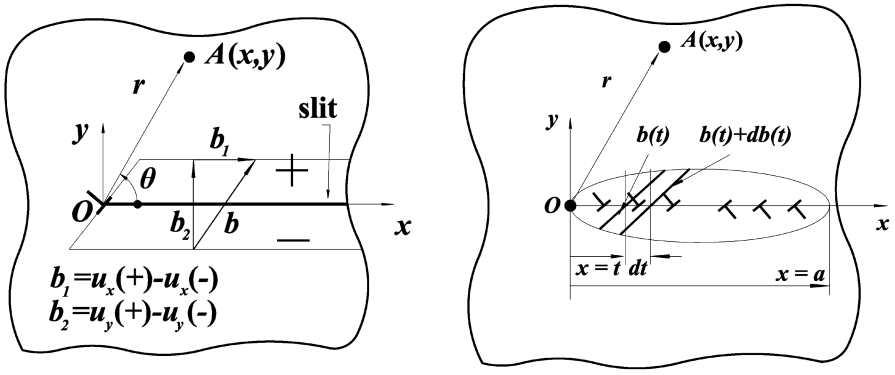

a) b)

Fig. 2 Definition of dislocation distributions: a) single dislocation at the origin producing a step opening with Burgers tangential (b_1) and normal (b_2) components extending from the origin to infinity along the x-axis, and b) distribution of dislocations representing the opening of a crack segment in an infinite plate.

interior. For simplicity of demonstration we have chosen a rectangular plate which can be modeled as four connected cracklike segments and with four wedges of 90 deg (but no crack tips). The problem is formulated in terms of integral equations expressed in terms of unknown edge dislocation distributions (EDDs) representing opening displacement profiles (ODPs) for the cracks [1–4] instead of influence functions based on crack line tractions [6], where an ODP is a vectorial plot of top to bottom distance between points originally coinciding on the faces of the undeformed crack segment under given boundary conditions (BCs); these can have both tangential and normal components (Fig. 2) in terms of Burgers vectors b_1 and b_2, respectively. To solve this boundary value problem (BVP) we employ the usual approach of superposition based on the dislocation distributions [9–11] method, which requires the determination of crack ODPs that satisfy the traction-free condition on interior crack faces and the given traction BCs on four exterior cracklike surfaces defining the rectangular plate boundary. Applying the method with a new point allocation scheme designed to reduce the number of evaluation points (Fig. 3) leads to a set of linear algebraic equations in terms of unknown weighting coefficients of ODP "building block" components. These components are crucial to representing appropriate physical crack behavior under the given BCs. These ODP components are categorized in terms of polynomial terms (t^n, $n = 0, 1, 2, \ldots$) and wedge terms ($t^{\rho+n}$, $0 < \rho < 1$) where t is a local coordinate directed along the crack line from a tip, a kink, or branch point, and ρ is a corresponding tip or material wedge eigenvalue as may occur at a kink or branch [12,13]. Once the coefficients of ODP components are solved for, one can easily calculate stress and displacement fields on the entire infinite body as well all SIFs at crack tips and wedges or kinks, not just those within the embedded rectangular plate, which happens to be the body of main interest. In other words two problems are solved, one byproduct being a rectangular hole in an infinite plate with tractions applied on the faces.

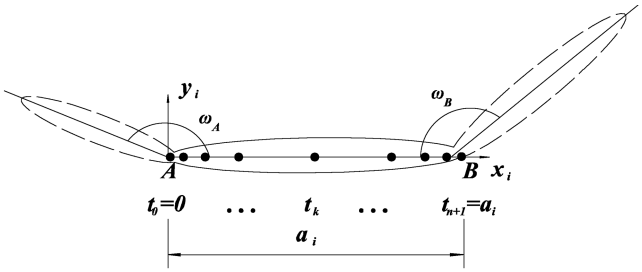

Fig. 3 Point allocation scheme.

A. Dislocation-Based Influence Fields

In the 2-D problems considered we construct certain ODPs, whose derivatives are EDDs, to ultimately generate crack-face tractions satisfying those prescribed in the BVP. The stress (σ) and displacement (u) fields induced by these EDDs are adapted from the description in Hills et al. [9] and Weertman [14], where we interpret the standard definition of the dislocation symbol to represent what is seen in Figs. 2a and 2b. These fields are given as follows:

$$\begin{Bmatrix} \sigma_{xx} \\ \sigma_{yy} \\ \sigma_{xy} \end{Bmatrix} = \frac{2G}{\pi(\kappa+1)r^4} \begin{bmatrix} (3x^2+y^2)y & -(x^2-y^2)x \\ -(x^2-y^2)y & -(x^2+3y^2)x \\ -(x^2-y^2)x & -(x^2-y^2)y \end{bmatrix} \begin{Bmatrix} b_1 \\ b_2 \end{Bmatrix}$$

$$r = \sqrt{x^2+y^2} \tag{1}$$

and

$$\begin{Bmatrix} u_x \\ u_y \end{Bmatrix} = \frac{1}{2\pi(\kappa+1)r^4} \times \begin{bmatrix} (\kappa+1)(\pi-\theta)-2xy/r^2 & -(\kappa-1)\ell_n(r/r_c)+2(x/r)^2 \\ -(\kappa-1)\ell_n(r/r_c)+2(y/r)^2 & (\kappa+1)(\pi-\theta)+2xy/r^2 \end{bmatrix} \begin{Bmatrix} b_1 \\ b_2 \end{Bmatrix} \tag{2}$$

and where $\kappa = 3-4\nu$ for plane strain, $\kappa = (3-\nu)/(1+\nu)$ for plane stress, and r_c is a constant said to be the "core" radius of the dislocation [14]. Note that the displacements have been interpreted in terms of taking limits in x and y approaching the bottom face from below or the top face from above, and θ is measured from the positive x-axis such that the dislocation shifts top and bottom faces symmetrically or antisymmetrically as appropriate relative to the x-axis. The preceding result also applies to an ED extending to the right of position t along the x-axis, upon replacing x by $(x-t)$.

Next we consider a single straight crack segment of length a, which is aligned along the x-axis of the present coordinate system and has its left end at the origin, i.e., along $0 < x < a$ and $y = 0$. We can use the preceding dislocation results to model the opening displacement as well as the stress and displacement fields around this crack segment. To do this we consider the superposition of an infinite number such EDs having infinitesimal Burgers vectors $\mathrm{d}b(t)$ of varying magnitude and with left endpoints now uniformly and continuously distributed in the distance variable t along the crack line segment as measured from the left end. Note that to represent the ODP of a crack, as shown in Fig. 2b, the infinitesimal Burgers vectors must change sign on the right half relative to the left half to close down the crack at the right end. The infinitesimal distribution of Burgers vectors is captured in the dislocation distribution weighting function defined as

$$\mu(t) = \frac{\mathrm{d}b(t)}{\mathrm{d}t} \tag{3}$$

Replacing b by $\mathrm{d}b(t)$ in Eqs. (1) and (2) (taking care to properly treat jump conditions at crack segment ends with the appropriate delta functions) and integrating in t along the crack segment directly yields the stress and displacement fields resulting from the crack segment ODP. These can be written in complex form ($z = x + iy$) as

$$\begin{Bmatrix} \sigma_{xx} \\ \sigma_{yy} \\ \sigma_{xy} \end{Bmatrix} = \frac{2G}{\pi(\kappa+1)r^4} \begin{bmatrix} \mathrm{Re}\{Z_2^1\} + y\mathrm{Im}\{Z_1^1\} - y\mathrm{Re}\{Z_1^2\} \\ \mathrm{Re}\{Z_2^1\} + y\mathrm{Im}\{Z_2^2\} - y\mathrm{Re}\{Z_1^2\} \\ y\mathrm{Re}\{Z_2^2\} + \mathrm{Re}\{Z_1^1\} - y\mathrm{Im}\{Z_1^1\} \end{bmatrix} \tag{4}$$

and

$$\begin{Bmatrix} u_x \\ u_y \end{Bmatrix} = \frac{1}{2\pi(\kappa+1)} \times \begin{Bmatrix} (1-\kappa)\mathrm{Re}\{Z_2^0\} - (\kappa+1)\mathrm{Im}\{Z_1^0\} + 2y\mathrm{Im}\{Z_2^1\} - 2y\mathrm{Re}\{Z_1^1\} \\ (\kappa-1)\mathrm{Re}\{Z_1^0\} - (K+1)\mathrm{Im}\{Z_2^0\} + 2y\mathrm{Re}\{Z_2^1\} + 2y\mathrm{Im}\{Z_1^1\} \end{Bmatrix} \tag{5}$$

where

$$Z_j^0 = \int_0^a \frac{b_j(t)}{z-t}\,\mathrm{d}t, \qquad Z_j^1 = \int_0^a \frac{\mu_j(t)}{z-t}\,\mathrm{d}t$$
$$Z_j^2 = \int_0^a \frac{\mu_j(t)}{(z-t)^2}\,\mathrm{d}t, \qquad (j = 1, 2) \tag{6}$$

For the power series basis terms we use to model crack segment ODPs, the crucial details of which we describe shortly, all integrals in Eq. (6) can be evaluated in closed form as given by Burton and Phoenix [1], TerMaath [2], TerMaath et al. [3], and Yavuz et al. [4]. These results are the foundation to developing the solution method.

B. Satisfaction of Traction BCs Along Crack Faces

In a typical multicrack problem there will be many crack segments that must be indexed by $i = 1, \ldots, C$ where C is the total number, and these segments may have different lengths and geometric orientations. They will be interconnected and treating them as a system will require working both in terms of local x–y coordinate systems for the individual crack segments and a global X–Y coordinate system for the overall crack system in the infinite plate. This must be kept in mind in developing the solution.

To satisfy the traction-free condition on each interior crack within the polygon-shaped finite plate as well as the prescribed tractions (from the plate loading) on each exterior crack segment, which are the cuts along the outer boundary of the finite plate, in the actual BVP (Fig. 1), the tractions must sum to zero on interior cracks and sum to the prescribed traction values along all exterior plate boundary surfaces, as seen in Fig. 1. Letting T_1 and T_2 denote the tangential and normal crack-face tractions, respectively, then in terms of the global coordinate system X–Y, we have for the crack-face tractions

$$\begin{cases} T_1 = n_X \sum_{i=1}^{c} \sigma_{XX}^{(i)} + n_Y \sum_{i=1}^{c} \sigma_{XY}^{(i)} = \begin{cases} n_X\sigma_{XX}^* + n_Y\sigma_{XY}^*, & \text{on exterior cut surfaces representing the finite plate boundaries} \\ 0, & \text{on interior crack surfaces} \end{cases} \\ T_2 = n_X \sum_{i=1}^{c} \sigma_{XY}^{(i)} + n_Y \sum_{i=1}^{c} \sigma_{YY}^{(i)} = \begin{cases} n_X\sigma_{XY}^* + n_Y\sigma_{YY}^*, & \text{on exterior cut surfaces representing the finite plate boundaries} \\ 0, & \text{on interior crack surfaces} \end{cases} \end{cases} \tag{7}$$

The left side of Eq. (7) shows the tractions coming from summing the contributions of all dislocation distributions representing plate boundary cuts and interior cracks. The right side of Eq. (7) represents the prescribed traction values on plate boundary cuts and interior crack surfaces. The two sides must balance. Note that, using the appropriate stress transformations, the traction components expressed in global X–Y coordinates must be derived from the stress components given by Eq. (4) in local coordinates x_i–y_i for each crack segment where evaluation of the integrals (in closed form) occurs. These evaluations occur at a specific set of allocation points along the interior crack faces or exterior cuts in question and are described in terms of the local coordinate system. For each local coordinate system x_i–y_i these traction components must be transformed to the global coordinate system X–Y before summation in (7).

C. Construction of Power Series for Approximating ODPs

Next we describe the approximating basis functions used to represent the tangential and normal ODPs denoted, respectively, as $b_1^{(i)}(t)$ and $b_2^{(i)}(t)$ in local coordinates, corresponding to the individual crack segments or cuts $i = 1, \ldots, C$. The ODP of a given crack segment or cut requires a representation in terms of special power series emanating from each end and terminating smoothly at

the opposite end. In the individual terms of these power series, the noninteger exponents, denoted by ρ, are certain eigenvalues that arise from the solution of classical wedge problems [12,13] associated with wedges at the segment ends that have singular stresses. Thus, these ρ values are real and satisfy $1/2 < \rho < 1$. Such singular wedges occur at crack tips and kinks and may also occur at branches. Therefore, at the end of each crack segment there could be none, one, or two applicable values depending on the values of the associated wedge angles. At a kink there will be one or two, but at a branch it is possible to have none, i.e., no singular stresses.

When they occur, such stress singularities are associated with two possible types of wedge distortions: symmetric mode I (smallest ρ value) and an antisymmetric mode II (next smallest ρ value). At a segment end, the number of such exponents associated with singular stresses depends on the adjoining wedge angle, ω (the angle encompassing the wedge material is $2\pi - \omega$ as in Fig. 3). For $0.57\pi < \omega < \pi$ there is only one such ρ value and it is associated with a mode I singularity. [A mode II distortion occurs but it is not singular as the eigenvalue (real part) exceeds unity.] For $0 < \omega < 0.57\pi$ there are two such ρ values, the larger associated with a mode II singularity and the smaller with a mode I singularity. For $\omega = 0$, corresponding to a crack tip both mode I and mode II ρ values are $1/2$.

The eigenvalues 0 and 1 also occur and are very important in treating the BVP. The first, 0, corresponds to wedge translation (normal and tangential) in terms of constant displacements. The second, 1, plays three roles: The first and more obvious role is wedge rotation about its tip, and this involves equal and opposite normal wedge surface displacements that are linear in distance from the wedge tip. The second role of the eigenvalue 1 involves more subtle forms of wedge distortion such as linear tangential displacements of the wedge surfaces. The third role is similar to the first but involves linear normal displacements of the wedge surfaces that generate wedge angle changes. All these possible types of distortions are accommodated in the polynomial series introduced next, as discussed by Burton and Phoenix [1].

For wedges with singular stresses there are also an infinite number of eigenvalues exceeding 1 in magnitude and these may be real or complex depending on the angle $\omega < \pi$ (where the real parts also exceed 1). The mating wedges, while having no singular stresses, also have an infinite number of eigenvalues (other than 0, or 1) that are possibly complex but have real parts exceeding 1. A stumbling block to considering complex eigenvalues directly is that integrals resulting from them cannot be treated in closed form. However, none of these eigenvalues involve singularities and we find the solution process to be more efficient and stable if we approximate their associated wedge distortions either with polynomial terms, or higher-order power terms based on ρ plus an integer, as is done next.

One final and subtle point is that despite the fact that there may be no singularities in the finite plate along its boundary, the opening displacements along the cuts representing the plate boundaries must include singular basis terms, because these happen to be needed for the corners in exterior, infinite plate that will be singular. For a cracked rectangular plate loaded in simple tension, for instance, the finite plate corners are not singular, but the infinite plate matching corners are 90 deg singular wedges in both modes I and II.

The ODP series for a given crack segment or boundary cut, i, is built up from power functions using all the preceding exponents depending on the adjoining wedge angles, and is written next in terms of distance t along its crack line measured from its left end in the context of Fig. 2. Its ODP series takes the form

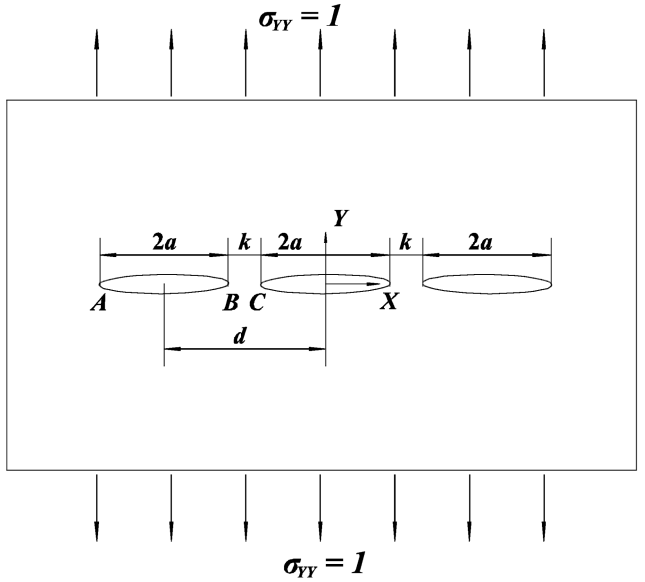

Fig. 4 Three collinear cracks in a finite plate under unit tension.

$$b_j^{(i)}(t) = P_j^{A(i)}(t/a_i) + W_{\rho_1^A j}^{A(i)}(t/a_i) + W_{\rho_2^A j}^{A(i)}(t/a_i) + P_j^{B(i)}(1 - t/a_i) + W_{\rho_1^B j}^{B(i)}(1 - t/a_i) + W_{\rho_1^B j}^{B(i)}(1 - t/a_i) \quad (8)$$

where

$$\begin{cases} P_j(\eta) = \sum_{k=0}^{N-2} p_{jk}[\eta^k - (N-k)\eta^{(N-1)} + (N-k-1)\eta^N] \\ W_{\rho j}(\eta) = \sum_{k=0}^{N-2} w_{\rho jk}[\eta^{(\rho+k)} - (N-k)\eta^{(\rho+N-1)} + (N-k-1)\eta^{(\rho+N)}] \end{cases} \quad (9)$$

As mentioned the ρ eigenvalues are accurately approximated by rational numbers (fractions) to allow closed form evaluation of the integrals in Eq. (6) which are given by Burton and Phoenix [1], TerMaath [2], TerMaath et al. [3], and Yavuz et al. [4] for various terms in Eq. (9).

D. Solution for Unknown Weighting Coefficients of Power Terms Approximating ODPs

Upon evaluating all the integrals in Eq. (6) arising from the ODP power series in Eq. (9) and substituting the results into Eqs. (4) and (5), we obtain expressions for the stress and displacement fields associated with the ith crack segment in the absence of all other crack segments and in local coordinates. Superposition of these series solutions for all segments and cuts, i.e., for $i = 1, \ldots, C$ yields an extremely accurate approximate solution to the BVP, provided all the coefficient values for terms in the various series are specifically chosen so as to satisfy as closely as possible the prescribed crack surface traction condition (which are zero on interior crack surfaces and prescribed values along plate boundary cuts) on each crack segment in the full system, as given by Eq. (7).

This approximate traction matching is actually done at an arbitrary but carefully chosen set of allocation points along each crack segment, none of which are at crack tips, kinks, or branch points, as illustrated in Fig. 3. The tractions are minimized in a mean-square sense by adjusting the coefficient weights in the full solution, and this

Table 1 Normalized SIFs (K_I/K_I^0) for three collinear cracks in a large finite square plate

	Tip A			Tip B			Tip C		
k/a	Exact	Other	Present	Exact	Other	Present	Exact	Other	Present
1/2	1.1103	1.1102[FEM]	1.1105	1.2835	1.2840[FEM]	1.2836	1.3214	1.3218[FEM]	1.3215
2/9	1.1644	1.1632[BEM]	1.1645	1.5645	1.5587[BEM]	1.5647	1.6068	1.6007[BEM]	1.6070
1/20	1.2587	1.2637[MKM]	1.2581	2.5185	2.5941[MKM]	2.5165	2.5537	2.6252[MKM]	2.5516

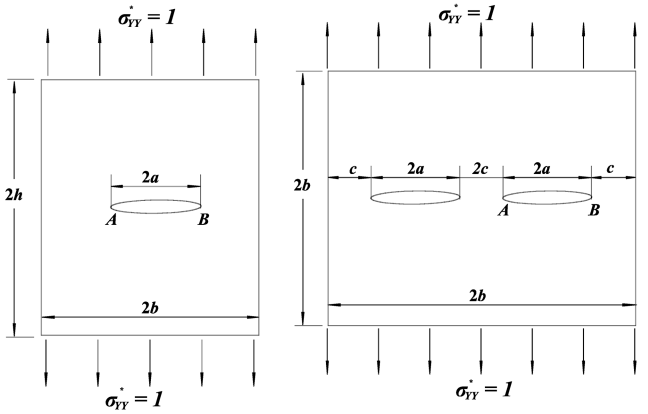

a) b)

Fig. 5 a) A single crack in a rectangular plate under unit tension, b) two collinear cracks in a square finite plate under unit tension.

requires a least-squares solution of a set of linear algebraic equations in terms of these unknown weighting coefficients. One added benefit is that we can determine an error estimate of how well the tractions calculated by the method actually match those prescribed. It also turns out to be beneficial to allocate increased numbers of points near the end points of segments when material singularities exist there.

Points are allocated according to the singularities occurring at the ends of the crack segment (Fig. 3) is the union of three sets of points allocated along the crack segment. Two sets collect points around singular end points and one set is for equally spacing to handle middle points' contributions . These sets are

$$\begin{cases} t_k = a_i\left(\frac{k}{n+1}\right)^4 \\ t_k = a_i\left[1-\left(\frac{k}{n+1}\right)^4\right], \quad k=1,2,\ldots,n \\ t_k = a_i\left(\frac{k}{n+1}\right), \end{cases} \tag{10}$$

where n is the total number of allocation points for each set (Fig. 3).

III. Results and Discussion

Stress intensity factors at both crack tips and wedge locations are obtained with the weighting coefficients of the corresponding terms inducing singular behavior. At the crack tips ($\rho = 1/2$), for the mode I and mode II stress intensity factors, K_I and K_{II}, respectively, are given by [2–4]

$$\begin{Bmatrix} K_I \\ K_{II} \end{Bmatrix} = \frac{2G}{1+\kappa}\sqrt{\frac{\pi}{2a}}\begin{Bmatrix} w_{\frac{1}{2}20} \\ w_{\frac{1}{2}10} \end{Bmatrix} \tag{11}$$

and at kink ends they become [2–4]

Table 3 Normalized SIFs (K_I/K_I^0) at crack tips A and B for two collinear cracks in a square finite plate

	Tip A			Tip B		
$2a/b$	0.1	0.4	0.7	0.1	0.1	0.7
Present	1.0054	1.0964	1.4015	1.0053	1.0938	1.3766
Chen et al. [5]	1.0054	1.0989	1.4269	1.0053	1.0919	1.3603

$$\begin{Bmatrix} K_I \\ K_{II} \end{Bmatrix} = -\frac{4G\pi}{1+\kappa} \times \begin{Bmatrix} \frac{\rho_1(1+\rho_1)}{(2\pi a)^{\rho_1}\sin[(\rho_1-1)(2\pi-\omega/2]}\left[1-\frac{(\rho_1-1)\sin[(\rho_1-1)(2\pi-\omega)/2]}{(\rho_1+1)\sin[(\rho_1+1)(2\pi-\omega)/2]}\right]w_{\rho_1 20} \\ \frac{\rho_2(1+\rho_2)}{(2\pi a)^{\rho_2}\sin[(\rho_2-1)(2\pi-\omega/2]}\left[\frac{(\rho_2-1)\sin[(\rho_2-1)(2\pi-\omega)/2]}{(\rho_2+1)\sin[(\rho_2+1)(2\pi-\omega)/2]}-\frac{\rho_2-1}{\rho_2+1}\right]w_{\rho_2 10} \end{Bmatrix} \tag{12}$$

Note that K_{II} at the kink becomes irrelevant when the second eigenvalue which is less than 1 does not exist for certain wedge angles. The following results are obtained for plane stress problems with $\nu = 0.3$. In calculations, $20 + 20 + 20 = 60$ allocation points ($n = 20$) and five polynomial and five wedge terms ($N = 5$) are taken unless otherwise stated.

A. Verification Samples

Results are obtained first for three collinear cracks (crack lengths are two units) in a large finite square plate (400×400) in Fig. 4 to see the agreement with SIFs of cracks in an infinite plate (normalized with $K_I^0 = \sigma_{YY}^*\sqrt{\pi a}$, the SIF of a single crack in an infinite plate under far-field tension) and compared with exact (, p. 169) (by Mushkelishvili's method) MKM [6], FEM [7], and BEM [8] results (Table 1). Seven crack segments are used. Even if cracks are very close, the present method gives very accurate results.

The second verification example involves a single crack in a rectangular finite plate under unit tension (Fig. 5a). Results are compared with Isida's [16] results (based on Laurent expansions of the complex potentials) for various plate aspect ratios and crack size ratios in Table 2. Stable results are obtained for $50 + 50 + 50 = 150$ allocation points ($n = 50$) and seven polynomial and seven wedge terms ($N = 7$). Increasing these numbers is necessary for analyzing very close crack tip and plate side interactions. If the interactions are weak, the desired accuracy can be achieved even with $n = 10$ and $N = 5$. Note that the present method is capable of considering different loading configurations.

Then, the problem of two collinear cracks in a finite square plate (six crack segments) is solved to compare results with those from a recent study which is the singular integral equation method using complex potentials by Chen et al. ([5], p. 118) (Fig. 5b and Table 3). As seen in Table 3, as cracks get closer, differences between the two methods slightly increase. In the light of previous verification results we can safely claim that the present method is more accurate than the other method. Again, even if the plate is small (for $2a/b = 0.7$, $a = 1$, $b = 20/7$, $c = 3/7$) the present method works extremely well.

The last verification example is an original one: One single branched Y-crack in a finite plate under unit tension (Fig. 6). Because

Table 2 Normalized SIFs (K_I/K_I^0) of Isida's approximate analytical method [16] and the present method at the crack tip A for a single crack in a rectangular finite plate

	$h/b = 0.4$		$h/b = 0.7$		$h/b = 1.0$		$h/b = 1.8$	
a/b	Isida [16]	Present	Isida [16]	Present	Isida [16]	Present	Isida [16]	Present
0.2	1.256	1.2529	1.103	1.1028	1.055	1.0554	1.025	1.0254
0.4	1.843	1.8413	1.400	1.3998	1.216	1.2160	1.112	1.1108
0.7	3.67	3.6610	2.19	2.1840	1.68	1.6643	——	1.4132
0.8	——	4.9348	——	2.4539	——	1.8474	——	1.4842

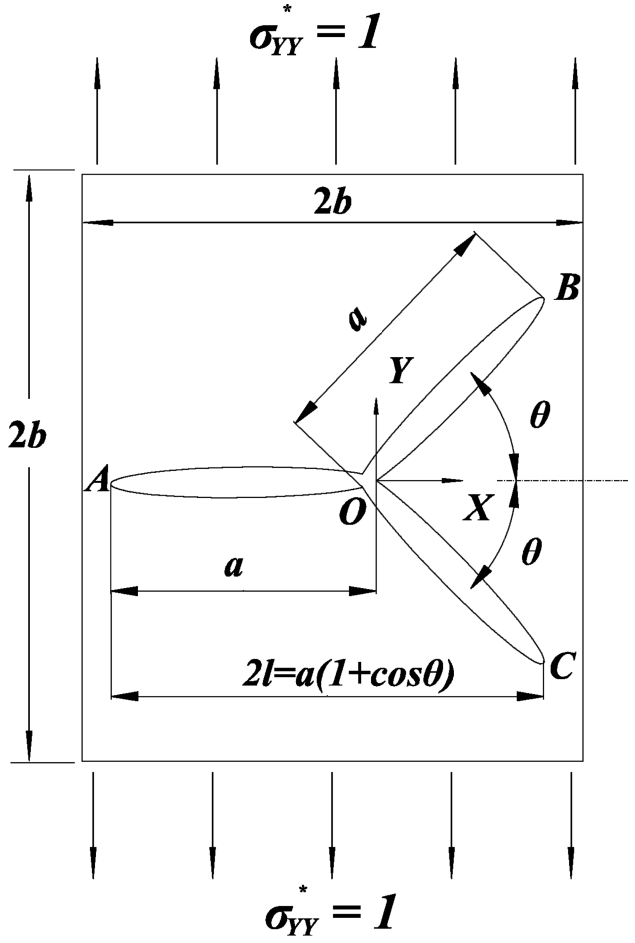

Fig. 6 A branched Y-crack in a finite rectangular plate under unit tension.

we only have results for infinite plates, comparisons with other methods such as Fredholm integral equation method (FIE) by Englund [17] and FEM by Daux et al. [18] have been made with the infinite plates in Table 4. Then, for a large finite plate the agreement is shown and SIFs are presented for different plate sizes and crack branch angles using $n = 50$ and $N = 7$ to get stable results.

B. Multiple Closely Interacting Cracks in a Finite Plate Under Combined Loading

After verifying the present method with some test configurations we present here a very complicated crack geometry involving kink and branch points and closely interacting with other cracks and plate boundaries in a finite plate under normal and shear loads. This sample having interacting skewed single cracks and kinked and branched cracks is shown in Fig. 7 and related results are presented in Tables 5 and 6 with the coordinates of tip and kink points of cracks. Tip A's location is chosen as reference point (0,0) and placed at the vertical midline of the plate. All segments have unit length and the plate is subjected to general loading which is unit biaxial tension and shear. Calculations in each case took less than 20 min in a notebook PC (P IV, 2.4 MHz CPU, 512 MB RAM) with MATLAB R14.

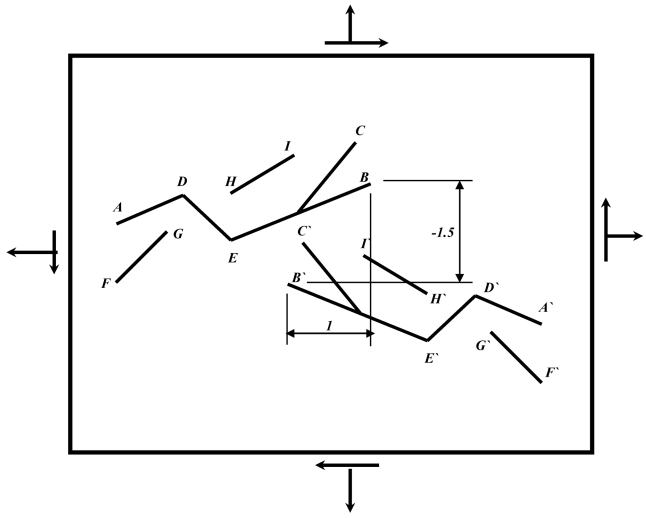

Fig. 7 Interacting multiple skewed, kinked, and branched cracks in a finite plate under unit biaxial tension and shear loads.

Far endpoints of cracks A and A' are affected when the size of the plate gets smaller. For a large-size plate (400×400) results converge to the infinite plate case. Because the wedge angles at D and E

Table 4 Normalized SIFs for a branched Y-crack in a finite square plate ($F_{I,II} = K_{I,II}/\sigma^*_{YY}\sqrt{\pi l}$))

	$\theta = 15$ deg		$\theta = 30$ deg		$\theta = 45$ deg	
a/b	F_I	F_{II}	F_I	F_{II}	F_I	F_{II}
∞	0.7368	0.1147	0.6583	0.3428	0.4948	0.5059
(FIE [17])	0.7367	0.1146	0.6583	0.3428	0.4948	0.5059
(FEM [18])	0.750	0.123	0.659	0.344	0.493	0.504
200	0.7367	0.1146	0.6584	0.3428	0.4948	0.5059
5	0.7812	0.1280	0.6971	0.3764	0.5186	0.5568
2.5	0.9126	0.1665	0.8184	0.4712	0.6162	0.7028
1.5	1.2177	0.2675	1.1453	0.6420	0.9875	0.9902

Table 5 SIFs at tip and kinked points of the left-side crack

Tip and kink points		A	B	C	D	E	F	G	H	I
Coordinates		(0, 0)	[3 cos(π/9) + cos(2π/9), 3 sin(π/9) − sin(2π/9)]	[2 cos(π/9) + cos(2π/9) + cos(5π/18), 2 sin(π/9) − sin(2π/9) + sin(5π/18)]	[cos(π/9), sin(π/9)]	[cos(π/9) + cos(2π/9), sin(π/9) − sin(2π/9)]	(0, −1)	[cos(π/4), −1 + sin(π/4)]	[cos(π/9) + cos(2π/9), sin(π/9)]	[cos(π/9)+ cos(2π/9)+ cos(π/6), sin(π/9) + sin(π/6)]
SIFs	Plate size									
K_I	∞	1.5727	1.7632	−1.4325	1.9562	0.7445	0.0418	−0.4761	−0.0507	−0.1787
	400×400	1.5732	1.7642	−1.4315	1.9576	0.7318	0.0453	−0.4755	−0.0505	−0.1784
	40×40	1.6270	1.8181	−1.4996	1.9596	0.6741	0.0417	−0.4943	−0.0508	−0.1826
	20×20	1.7943	1.9932	−1.6920	1.9587	0.4951	0.0510	−0.5317	−0.0517	−0.1933
	10×10	2.3679	2.8156	−2.2819	1.8315	−0.2144	0.1192	−0.5890	−0.0469	−0.2054
K_{II}	∞	2.6044	2.1979	−0.1936	N/A	N/A	0.1695	0.0859	−0.2359	−0.0391
	400×400	2.6041	2.1976	−0.1935	N/A	N/A	0.1695	0.0855	−0.2362	−0.0393
	40×40	2.6727	2.2483	−0.1783	N/A	N/A	0.1998	0.1119	−0.2267	−0.0239
	20×20	2.8522	2.4042	−0.1337	N/A	N/A	0.2894	0.1885	−0.1979	0.0213
	10×10	3.3671	3.0394	0.0391	N/A	N/A	0.4832	0.3974	−0.0653	0.1949

Table 6 SIFs at tip and kinked points of the right-side crack, which is a mirror image of the left-side crack

Tip and kink points SIFs	Plate size	A'	B'	C'	D'	E'	F'	G'	H'	I'
K_I	∞	3.3516	2.2993	5.0671	−1.0077	6.0691	4.0134	3.4298	0.3770	0.9163
	400×400	3.3517	2.2983	5.0667	−1.0060	6.0699	4.0134	3.4299	0.3777	0.9174
	40×40	3.4425	2.3864	5.1453	−1.0427	6.2356	4.0882	3.4882	0.3867	0.9382
	20×20	3.7215	2.6700	5.3966	−1.1160	6.7489	4.3255	3.6812	0.4157	1.0043
	10×10	4.9887	3.9992	6.5819	−1.2164	9.1497	5.2782	4.6257	0.5498	1.3034
K_{II}	∞	2.2122	0.9419	−0.0001	N/A	N/A	−0.0528	0.9434	−0.2977	0.1356
	400×400	2.2119	0.9424	−0.0002	N/A	N/A	−0.0559	0.9437	−0.2974	0.1355
	40×40	2.2383	0.9625	−0.0278	N/A	N/A	−0.0848	0.9380	−0.3208	0.1184
	20×20	2.3379	1.0248	−0.1143	N/A	N/A	−0.1661	0.9279	−0.3947	0.0648
	10×10	3.0029	1.2449	−0.4645	N/A	N/A	−0.5041	0.9168	−0.7070	−0.1499

smaller than the critical angle mentioned before, mode II behavior does not take place. As the size of the plate gets smaller, cracks get closer to the edge and therefore, SIFs at these points get larger. Even at some points such as C, E, I, and I', they change their signs.

IV. Conclusion

Interactions of multiple cracks of complex shapes in finite plates are analyzed with a method based on superposition and dislocation distribution theory. It is verified that the presented method is very efficient and fast to determine SIFs, stress, and displacement fields in finite plates because the approximation functions of ODPs represent physically realistic behavior of cracks. It is possible to solve very complex multicrack problems which are a combination of single straight and skewed cracks, branched Y-cracks, kinked V-cracks in a rectangular plate under various loading conditions including getting SIFs, and singularity exponents for wedge tips, which may be sources of crack branching. Different shapes and different loading conditions for finite plates involving multicracks can be analyzed. For future works, curved cracks are also applicable for either exterior or interior cracks with this method.

References

[1] Burton, J. K., Jr., and Phoenix, S. L., "Superposition Method for Calculating Singular Stress Fields at Kinks, Branches and Tips in Multiple Crack Arrays," *International Journal of Fracture*, Vol. 102, No. 2, 2000, pp. 99–139.

[2] TerMaath, S., "A Two-Dimensional Analytical Technique for Studying Fracture in Brittle Materials Containing Interacting Kinked and Branched Cracks," Ph.D. Dissertation, Civil Engineering Dept., Cornell Univ., Ithaca, NY, 2000.

[3] TerMaath, S. C., Phoenix, S. L., and Hui, C-.Y., "A Technique for Studying Interacting Cracks of Complex Geometry in 2-D," *Engineering Fracture Mechanics*, 2006 (in press).

[4] Yavuz, A. K., Phoenix, S. L., and TerMaath, S. C., "An Accurate and Fast Analysis for Strongly Interacting Multiple Crack Configurations Including Kinked (V) and Branched (Y) Cracks," *International Journal of Solids and Structures*, 2006 (in press).

[5] Chen, Y. Z., Hasebe, N., and Lee, K. Y., *Multiple Crack Problems in Elasticity*, WIT Press, Southampton, England, U.K., 2003.

[6] Li, Y. P., Tham, L. G., Wang, Y. H., and Tsui, Y., "A Modified Kachanov Method for Analysis of Solids with Multiple Cracks," *Engineering Fracture Mechanics*, Vol. 70, No. 9, 2003, pp. 1115–1129.

[7] Dong, Y. F., and Denda, M., "Computational Modeling of Elastic and Plastic Multiple Cracks by the Fundamental Solutions," *Finite Elements in Analysis and Design*, Vol. 23, Nos. 2–4, 1996, pp. 115–132.

[8] Denda, M., "Mixed Mode I, II and III Analysis of Multiple Cracks in Plane Anisotropic Solids by the BEM: A Dislocation and Point Force Approach," *Engineering Analysis with Boundary Elements*, Vol. 25, Nos. 4–5, 2001, pp. 267–278.

[9] Hills, D., Kelly, P., Dai, D., and Korsunsky, A., *Solution of Crack Problems: The Distributed Dislocation Technique*, Kluwer Academic Publishers, Dordrecht, The Netherlands, 1996.

[10] Hirth, J., and Lothe, J., *Theory of Dislocations*, John Wiley & Sons, New York, 1982.

[11] Lardner, R., *Mathematical Theory of Dislocations and Fracture*, Univ. of Toronto Press, Great Britain, 1974.

[12] Williams, M., "Stress Singularities Resulting from Various Boundary Conditions in Angular Corners of Plates in Extension," *Journal of Applied Mechanics*, Vol. 19, No. 4, 1952, pp. 526–528.

[13] Williams, M., "On the Stress Distribution at the Base of a Stationary Crack," *Journal of Applied Mechanics*, Vol. 24, No. 1, 1957, pp. 109–114.

[14] Weertman, J., *Dislocations Based Fracture Mechanics*, World Scientific Publishing, Singapore, 1996.

[15] Tada, H., *The Stress Analysis of Cracks Handbook*, 3rd ed., ASME Press, New York, 2000.

[16] Isida, M., "Effect of Width and Length on Stress Intensity Factors of Internally Cracked Plates Under Various Boundary Conditions," *International Journal of Fracture*, Vol. 7, No. 3, 1971, pp. 301–316.

[17] Englund, J., "Stable Algorithm for the Stress Field Around a Multiply Branched Crack," *International Journal for Numerical Methods in Engineering*, Vol. 63, No. 6, 2005, pp. 926–946.

[18] Daux, C., Mos, N., Dolbow, J., Sukumar, N., and Belytschko, T., "Arbitrary Branched and Intersecting Cracks with the Extended Finite Element Method," *International Journal for Numerical Methods in Engineering*, Vol. 48, No. 12, 2000, pp. 1741–1760.

B. Sankar
Associate Editor